WA-001

J. Chem. Thermodynamics **1994**, 26, 155–163

The vapor pressure, infrared spectrum, and thermodynamic properties of ZrF_4(g)

R. J. M. Konings

Netherlands Energy Research Foundation, ECN, P.O. Box 1, 1755 ZG, Petten, The Netherlands

and D. L. Hildenbrand

SRI International, Menlo Park, California 94025, U.S.A.

(Received 27 April 1993; in final form 23 July 1993)

The vibrational spectrum of ZrF_4 in the gas phase was measured by high-temperature infrared spectroscopy. The spectrum showed two strong bands which were assigned to the asymmetric stretching wavenumber $\tilde{\nu}_3$ and the asymmetric bending wavenumber $\tilde{\nu}_4$. From a correlation of the established i.r.-inactive wavenumbers in other MX_4 molecules with the i.r.-active values, the two i.r.-inactive modes in ZrF_4 were estimated with an expected accuracy of about $\pm 15\ cm^{-1}$. In addition, the vapor pressure of ZrF_4(c) was measured in the range 700 K to 850 K by the torsion-effusion technique, yielding for the equilibrium pressure p_e:

$$\lg(p_e/p^\circ) = -(11974 \pm 26)(T/K)^{-1} + (10.284 \pm 0.062),$$

where $p^\circ = 101.325$ kPa. The entropy of ZrF_4(g), derived from the second-law entropy of vaporization and the known entropy of the solid, is in close accord with the corresponding statistical value calculated from the vibrational wavenumbers and the reported structural parameters for tetrahedral ZrF_4, showing that the results are internally consistent. Enthalpies of sublimation and thermodynamic properties of ZrF_4(g) are reported.

1. Introduction

The entropies of gaseous compounds can be calculated from molecular quantities by means of statistical-thermodynamic procedures. For this purpose accurate data on the geometry, vibrational wavenumbers, and electronic states of the molecule are required. Vapor-pressure studies, in turn, yield thermodynamic quantities for the sublimation (or vaporization) process. By second-law treatment of the vapor pressures, the enthalpy and entropy of the reaction can be obtained from the slope and intercept of the (linear) vapor-pressure equation. Third-law treatment allows the calculation of the reaction enthalpy at a reference temperature for each point, using the entropies of the products and reactants. In case the entropy of the condensed phase is accurately known, it can be combined with the second-law entropy of sublimation to yield a vapor entropy that can be compared with statistically calculated values. Hildenbrand[1,2] has described this approach and shown how uncertain molecular parameters may be clarified with the aid of reliable equilibrium data. In the present paper this procedure is applied to ZrF_4, for which gas-phase infrared spectroscopy and torsion-effusion measurements have been made.

0021-9614/94/020155+09 $08.00/0

2. Experimental

Two different samples were employed for the measurements, one in each of our laboratories. The SRI sample was prepared from zirconium metal and HF(aq), dried in HF(g), and sublimed in an Ar stream in a monel tube. The ECN sample was prepared from hafnium-free zirconium metal dissolved in HF(aq). The precipitate ($ZrF_4 \cdot H_2O$) was dried in a stream of (Ar+HF)(g) at $T = 673$ K, using nickel equipment. The purities of the samples were checked by X-ray diffraction analysis, which did not show any impurities.

The infrared spectra were recorded at ECN with a BOMEM DA3.02 Fourier-transform spectrometer connected to a laboratory-built gas-cell (designation HTOC-2) which operates at high temperatures. Details of the equipment have been described in previous papers.[3,4] The following experimental arrangements were used for the operation of the spectrometer: for the wavenumber range 1000 cm^{-1} to 375 cm^{-1} a globar light source and a DTGS detector; and for the 375 cm^{-1} to 75 cm^{-1} range a Hg light source and a bolometer operating at $T = 4.2$ K. KRS5 or Si windows were used. The spectra were recorded at 0.5 cm^{-1} or 1 cm^{-1} resolution; 128 scans were co-added. The gas atmosphere in the cell was argon at a pressure of 1.5 kPa at room temperature. Loading of the cell was done in an argon-filled glove box.

The vapor pressure of ZrF_4 was measured at SRI by the torsion-effusion method, which has been fully described in earlier publications and references cited therein.[5] Essentially, the torsion-effusion apparatus is an effusion manometer in which the sample vapor pressure is determined from the geometrical constants of the effusion cell, the torsion constant of the suspension fiber, and the observed angular deflection of the cell at each temperature; all of these quantities can be measured directly and used to determine the vapor pressure in an absolute sense. In addition, the molar mass of the effusing vapor can be evaluated from simultaneous mass-loss measurements. Frequent checks with laboratory vapor-pressure standards (Ag, KCl) have shown that both absolute pressures and vapor molar masses are accurate to within 5 per cent.

Graphite cells were used for all measurements reported here. In order to corroborate a pronounced dependence of pressure on orifice size, several sets of torsion-Langmuir (free-surface) vaporization measurements were made by mounting pressed discs of ZrF_4 on a graphite holder, but off the suspension axis so that front-surface vaporization generated an angular displacement in the same fashion as molecular effusion. The ZrF_4 discs had a diameter of about 0.55 cm. Langmuir pressures were calculated from the exposed surface-areas of the discs and their perpendicular distance from the suspension axis.

3. The infrared spectrum of ZrF_4

The infrared spectrum of the vapor above ZrF_4 in the temperature range 950 K to 990 K showed two distinct absorption bands whose intensity was strongly

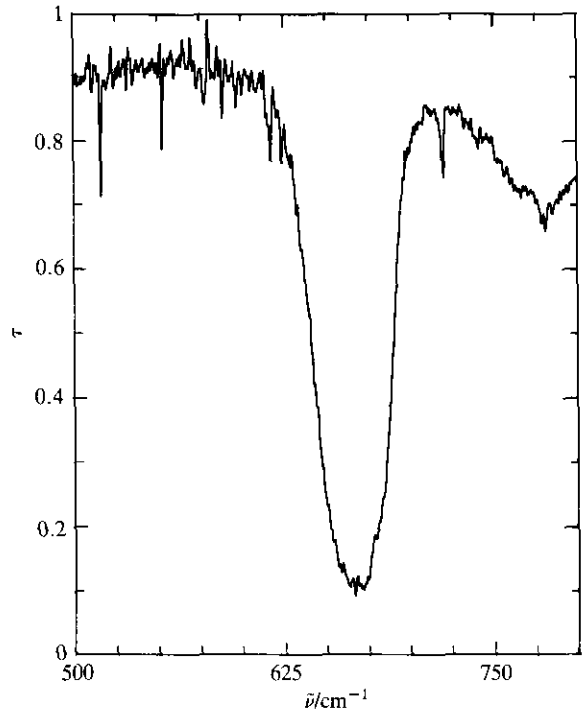

FIGURE 1. The $\tilde{\nu}_3$ band of ZrF_4(g): transmittance τ against wavenumber $\tilde{\nu}$.

temperature dependent. These bands are attributed to the ZrF_4 vapor species, being the asymmetric Zr–F mode $\tilde{\nu}_3$ and the F–Zr–F deformation mode $\tilde{\nu}_4$, respectively, for a tetrahedral geometry. The $\tilde{\nu}_3$ band is located at 668.0 cm^{-1} (figure 1), the $\tilde{\nu}_4$ band shows a clear PQR band structure at the lowest temperature with the central Q-branch at 178.6 cm^{-1}, the P-branch at 168.0 cm^{-1}, and the R-branch at 191.5 cm^{-1} (figure 2). From the separation of the P and R branches we can evaluate

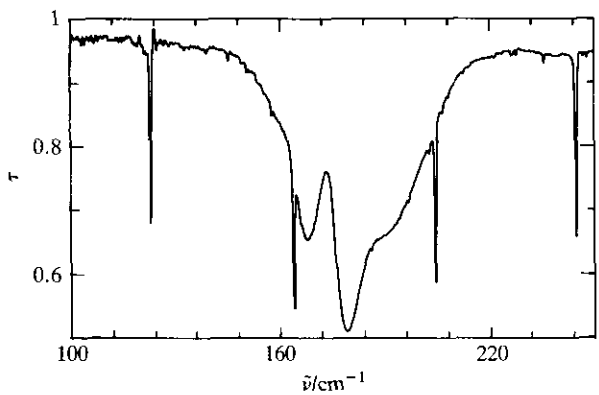

FIGURE 2. The $\tilde{\nu}_4$ band of ZrF_4(g): transmittance τ against wavenumber $\tilde{\nu}$.

the Coriolis constant ζ_4 using the equation:[6]

$$\Delta\tilde{\nu}_{PR} = 4(BkT/hc)^{1/2}(1-\zeta_4), \quad (1)$$

where B is the rotational constant and T is the thermodynamic temperature. Using $B = 0.04342\ cm^{-1}$ as calculated from the Zr–F internuclear distance as obtained by Girichev *et al.*[7] by gas-phase electron-diffraction measurements, we obtain $\zeta_4 = 0.13$.

The present result for the Zr–F stretching wavenumber $\tilde{\nu}_3$ is in excellent agreement with the value reported by Büchler *et al.*[8] as well as by Blander and Morgan,[9] who obtained $\tilde{\nu}_3 = 668\ cm^{-1}$ and $670\ cm^{-1}$, respectively. The value for $\tilde{\nu}_4$ is somewhat lower than reported by Büchler *et al.*, but these authors assigned a rather large uncertainty to their result. They estimated $\tilde{\nu}_4 = (190 \pm 20)\ cm^{-1}$ since only a wing of an absorption band was observed near the cut-off of the caesium-iodide prism. This value is in reasonable agreement with the position of the R-branch found here.

In addition to the values for the i.r.-active vibration bands of $ZrF_4(g)$, as obtained here, values for the i.r.-inactive $\tilde{\nu}_1$ and $\tilde{\nu}_2$ are needed for the calculation of the vibrational contribution to the thermal functions, but experimental determinations have not been reported. Girichev *et al.*[7] estimated the values from a combined analysis of their results from the electron-diffraction measurements and the results of Büchler *et al.* for the infrared-active vibrational modes. They thus obtained $\tilde{\nu}_1 = 627\ cm^{-1}$ and $\tilde{\nu}_2 = 182\ cm^{-1}$ when both $\tilde{\nu}_3$ and $\tilde{\nu}_4$ were included in the analysis. We here employ a more empirical method to derive the i.r.-inactive vibrational modes. As shown in figure 3, a linear relation exists between the $\tilde{\nu}_3$ and $\tilde{\nu}_1$ vibrational wavenumbers in other MX_4 molecules, representing the experimental to within

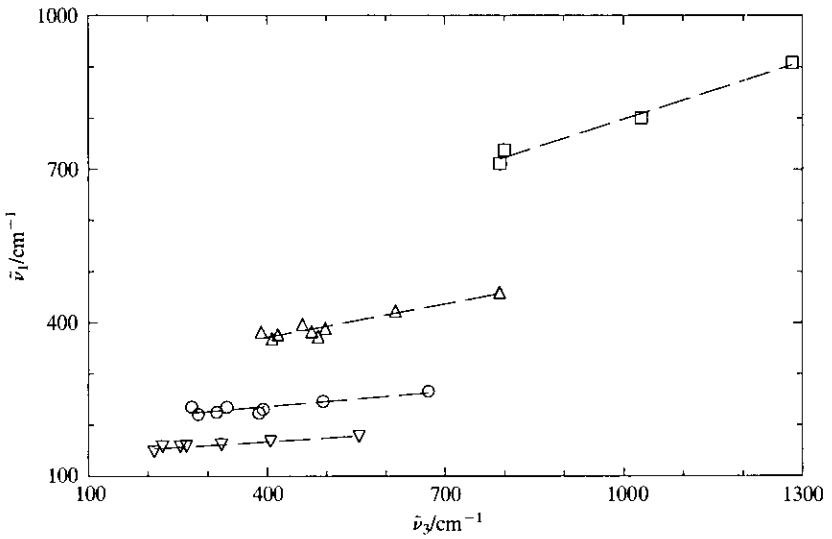

FIGURE 3. The relation between the $\tilde{\nu}_1$ and $\tilde{\nu}_3$ stretching wavenumbers in tetrahedral MX_4 metal halides; □, fluorides; △, chlorides; ○, bromides; ▽, iodides.

TABLE 1. Molecular quantities used in the statistical-thermodynamic calculations for ZrF_4(g)

Parameter	Value
Symmetry group	T_d
Symmetry number, σ	12
M/(g·mol^{-1})	167.2176
r(Zr–F)/nm	0·1883
$\tilde{\nu}_i$/cm^{-1} [a]	675, 156 (2), 668.0 (3), 178.6 (3)
$I_A I_B I_C$/(g^3·cm^6)	$2.6790\ 10^{-113}$
g_0	1

[a] Degeneracies in parentheses.

TABLE 2. The standard molar thermodynamic functions of ZrF_4(g)

($p^\circ = 101.325$ kPa; $\Phi_m^\circ \overset{\text{def}}{=} \Delta_0^T S_m^\circ - \Delta_0^T H_m^\circ/T$)

$\frac{T}{K}$	$\frac{C_{p,m}^\circ}{R}$	$\frac{\Delta_0^T S_m^\circ}{R}$	$\frac{\Phi_m^\circ}{R}$ [a]	$\frac{\Delta_{298.15K}^T H_m^\circ}{R\cdot K}$	$\frac{T}{K}$	$\frac{C_{p,m}^\circ}{R}$	$\frac{\Delta_0^T S_m^\circ}{R}$	$\frac{\Phi_m^\circ}{R}$ [a]	$\frac{\Delta_{298.15K}^T H_m^\circ}{R\cdot K}$
298.15	10.517	38.744	38.744	0	900	12.608	51.785	43.770	7214
300	10.537	38.809	38.744	19	1000	12.680	53.117	44.639	8478
400	11.367	41.965	39.169	1118	1200	12.775	55.438	46.251	11024
500	11.863	44.559	39.995	2282	1400	12.833	57.412	47.708	13586
600	12.172	46.751	40.943	3485	1600	12.872	59.129	49.031	16156
700	12.373	48.644	41.911	4713	1800	12.898	60.646	50.239	18733
800	12.511	50.306	42.859	5957	2000	12.917	62.006	51.349	21315

± 15 cm^{-1}. Extrapolation of the trend in the fluorides to ZrF_4 leads, with the present value for $\tilde{\nu}_3$, to the symmetric stretching mode $\tilde{\nu}_1 = 675$ cm^{-1}. Similarly, we obtain $\tilde{\nu}_2 = 156$ cm^{-1} from the correlation between $\tilde{\nu}_4$ and $\tilde{\nu}_2$. These results differ considerably from the values given by Girichev *et al.*, which only poorly agree with the noted trend.

The thermodynamic functions of gaseous ZrF_4, as used in the thermodynamic analysis of the vapor pressures, have been calculated from the vibrational wavenumbers derived here and the moment of inertia calculated from the internuclear distance of 0.1886 nm reported by Girichev *et al.* for a tetrahedral structure. The ground electronic state is assumed to be singlet, with no significant contributions from excited states. The selected molecular constants are listed in table 1; the resulting thermal functions calculated from these quantities are listed in table 2.

4. The vapor pressure of ZrF_4

The results of the torsion-effusion measurements, as listed in table 3, have been obtained with five different graphite cells of variable orifice area, which varied from 0.00215 cm^2 to 0.0280 cm^2. A moderate orifice-size effect is observed, correlating well with the Whitman–Motzfeldt model, which relates the measured and equilibrium pressures on the basis of cell geometry and the condensation coefficient.[10 12] The

TABLE 3. The vapor pressure of ZrF_4; $p^\circ = 101.325$ kPa; Ca, effective orifice area; p_T, observed pressure; p_e, equilibrium pressure

T/K	$10^6 \cdot (p_T/p^\circ)$	$10^6 \cdot (p_e/p^\circ)$
cell G-18, $Ca = 0.00215$ cm^2		
753.8	2.40	2.48
764.6	4.19	4.34
767.2	4.64	4.80
771.1	5.54	5.74
778.5	7.65	7.92
780.1	8.40	8.70
788.2	12.1	12.5
794.0	15.6	16.2
797.7	17.9	18.5
800.4	20.8	21.5
804.8	25.0	25.9
807.1	27.7	28.7
817.3	41.7	43.2
821.4	50.5	52.3
825.9	60.2	62.3
826.9	63.4	65.6
828.4	67.4	69.8
836.1	90.4	93.6
840.6	110.4	114.3
844.6	128.4	132.9
849.6	156.2	161.7
855.7	194.8	201.7
cell G-10, $Ca = 0.00970$ cm^2, run 1		
716.4	0.32	0.37
719.0	0.35	0.41
723.3	0.43	0.50
731.4	0.72	0.83
734.1	0.84	0.97
739.0	1.06	1.23
746.6	1.57	1.82
751.6	2.03	2.35
758.8	2.84	3.29
763.5	3.62	4.20
770.0	4.85	5.62
770.4	4.99	5.78
773.6	5.66	6.56
780.5	7.90	9.16
783.5	8.80	10.2
788.7	11.2	13.0
793.7	13.8	16.0
798.0	16.6	19.2
803.8	20.8	24.1
805.1	21.9	25.4
809.1[a]	26.2	30.4
809.3	25.9	30.0
813.2	31.2	36.2
816.7	34.1	39.5
819.8	40.1	46.5
cell G-10, $Ca = 0.00970$ cm^2, run 2		
706.8	0.19	0.22
719.9	0.37	0.43
723.2	0.44	0.51
724.8	0.51	0.59
728.1	0.59	0.68
732.6	0.73	0.85
736.0	0.86	1.00
745.6	1.41	1.63
752.9	1.98	2.29
752.9	2.04	2.36
768.4	4.14	4.80
769.8	4.52	5.24
774.5	5.43	6.30
777.4	6.28	7.30
783.2	8.12	9.41
787.1	9.72	11.3
787.5	9.80	11.4
792.6	12.0	13.9
795.9	13.8	16.0
799.0	15.9	18.4
806.2	21.3	24.7
817.7	33.9	39.3
817.9	34.1	39.5
823.1	41.9	48.6
cell G-14, $Ca = 0.0157$ cm^2		
719.6	0.32	0.40
727.9	0.51	0.64
733.9	0.72	0.91
742.7	1.13	1.42
745.5	1.28	1.61
753.8	1.91	2.40
767.2	3.59	4.51
767.3	3.56	4.48
768.0	3.74	4.70
768.1	3.76	4.73
777.8	5.55	6.98
782.7	7.04	8.85
786.9	8.44	10.6
792.2	10.8	13.6
792.4	10.8	13.6
792.5	10.9	13.7
796.1	12.5	15.7
801.6	15.1	19.0
815.3[a]	26.6	33.4
cell G-15, $Ca = 0.0207$ cm^2		
701.1	0.11	0.15
703.5	0.14	0.19
711.9	0.21	0.28
716.6	0.28	0.37
718.5	0.31	0.41
725.0	0.44	0.59
726.6	0.48	0.64
731.9	0.62	0.83
734.6	0.73	0.97
736.7	0.84	1.12
738.0	0.88	1.17
742.2	1.08	1.44
743.2	1.15	1.53
748.2	1.46	1.94
753.0	1.79	2.38
753.6	1.92	2.56
754.0	1.92	2.56
762.2	2.84	3.78
766.8	3.49	4.65
774.2	4.82	6.42
773.7	4.86	6.47
780.5	6.51	8.67
780.8	6.48	8.63
790.5	10.2	13.6
791.0	10.0	13.3
791.1	10.4	13.9
796.5	13.0	17.3
801.7	16.0	21.3
cell G-8, $Ca = 0.0280$ cm^2		
696.5	0.078	0.11
708.0	0.16	0.23
714.1	0.24	0.35
724.8	0.42	0.61
729.9	0.51	0.74
731.5	0.60	0.88
732.9	0.65	0.95
739.9	0.84	1.23
742.9	1.06	1.55
751.5	1.62	2.36
751.8	1.58	2.31
758.8	2.27	3.31
760.2	2.24	3.27
763.0	2.77	4.04
767.8	3.31	4.83
771.9	3.93	5.73
775.1	4.42	6.45
778.6	5.48	8.00
786.6	7.35	10.7
787.0	7.64	11.1
791.7	8.98	13.1
796.8	11.5	16.8

[a] Rejected on the basis of a statistical test.

experimental vapor pressures have been fitted to the equation:

$$p_e = p_T(1 + \beta Ca), \quad (2)$$

where p_e is the equilibrium pressure, p_T the observed pressure, Ca the effective orifice area (product of Clausing factor C and planar orifice area a), and β a parameter that is obtained as the slope of a plot of p_T^{-1} against Ca. From the present results we obtain for β the value 16.4 cm^{-2}. The equilibrium pressures calculated from this value are also included in table 4.

To a first approximation, $\beta = (\alpha A)^{-1}$ where α is the condensation coefficient and A the vaporization surface area. If A is taken to be the cross-sectional area of the effusion chamber, then $\alpha = 0.16$. This value is in good agreement with the ratio of Langmuir to effusion pressures measured here, which ranged from 0.1 to 0.2, showing that there is indeed a small kinetic barrier to the vaporization process and that the Whitman–Motzfeldt model provides a credible interpretation.

Seven mass-loss measurements in the temperature range 800 K to 825 K with another graphite cell G-6 yielded an average vapor molar mass of $(150 \pm 10)\ g \cdot mol^{-1}$, compared with that of $167.2\ g \cdot mol^{-1}$ for ZrF_4 monomer, confirming the monomeric character of the vapor.

The vapor pressures from the different graphite cells as well as the derived sublimation enthalpies are summarized in table 4. The third-law values are in good agreement, but the results from cells G-10 (run 2) and G-14 show a clear temperature trend, indicating that secondary effects may have occurred. Similarly, the second-law enthalpies reasonably agree with the third-law values except for cells G-10 (run 2) and G-14. On the basis of this analysis, the results of these runs have not been included in the final analyses.

The combined vapor pressures of cells G-18, G-10 (run 1), G-15, and G-8 can be represented by the equation:

$$\lg(p_e/p^\circ) = -(11974 \pm 26)(T/K)^{-1} + (10.284 \pm 0.062),$$

where $p^\circ = 101.325$ kPa.

From the results for the present study we calculate by third-law analysis $\Delta_{sub}H_m^\circ(298.15\ K) = (240.00 \pm 0.05)\ kJ \cdot mol^{-1}$, which is close to the second-law value $\Delta_{sub}H_m^\circ(298.15\ K) = (239.3 \pm 0.5)\ kJ \cdot mol^{-1}$, the quoted errors being the statistical values. The overall uncertainty in the third-law is estimated to be about

TABLE 4. Sublimation results for ZrF_4(s)

Cell	Ca/cm^2	n	T/K	$\lg(p_e/p^\circ) = (A \cdot K/T) + B$		$\Delta_{sub}H_m^\circ(298.15\ K)/(kJ \cdot mol^{-1})$	
				A	B	2nd law	3rd law
G-18	0.00215	22	754 to 856	−12013	10.338	240.9 ± 0.8	239.93 ± 0.04
G-10	0.00970	24	716 to 820	−11947	10.252	238.7 ± 1.2	239.95 ± 0.09
	0.00970	24	707 to 818	−11761	9.985	235.1 ± 0.1	240.33 ± 0.11
G-14	0.0157	24	720 to 815	−11737	9.942	234.5 ± 1.3	240.50 ± 0.12
G-15	0.0207	28	701 to 802	−11927	10.219	237.9 ± 0.8	240.02 ± 0.07
G-8	0.0280	22	697 to 797	−11843	10.104	236.7 ± 1.7	240.07 ± 0.15

TABLE 5. The molar enthalpy of sublimation of ZrF_4 at $T = 298.15$ K

Authors	T/K	Method[a]	$\Delta_{sub}H^\circ_m(298.15\ K)/(kJ \cdot mol^{-1})$ 2nd law	3rd law
Lauter[13]	913 to 1178	—[c]	236.7	240.75 ± 1.00
Sense *et al.*[14]	890 to 115	T	253.5 ± 0.4	241.81 ± 0.58
Cantor *et al.*[15]	983 to 1081	S	234.5 ± 2.6	239.81 ± 0.17
Galkin *et al.*[16]	713 to 873	—[c]	215.9	232.30 ± 1.16
Akashin *et al.*[17]	681 to 913	M	248.7	242.57 ± 1.70
Fischer and Petzel[18]	983 to 1177	B	240.6	241.11 ± 0.11
Sidorov *et al.*[19]	769	M	—	242.98
This study	696 to 856	TE	239.3 ± 0.5	240.00 ± 0.05

[a] T, transpiration method; S, static measurements; M, mass spectrometry; B, boiling-temperature method; TE, torsion-effusion.
[b] Statistical errors are given. [c] Not specified.

$\pm 1\ kJ \cdot mol^{-1}$, based on possible errors in the vapor pressures and the thermal functions of solid and gaseous ZrF_4; the corresponding uncertainty in the second-law value is estimated to be about $\pm 3\ kJ \cdot mol^{-1}$ from the reproducibility among runs and the routine comparison with known values for vapor-pressure standards. From the selected third-law enthalpy and the established properties of the solid phase,[20-22] one derives: $\Delta_f H^\circ_m(ZrF_4, g, 298.15\ K) = -(1671.2 \pm 1.0)\ kJ \cdot mol^{-1}$. For the second-law entropy of reaction we obtain $\Delta_{sub}S^\circ_m(772.8\ K) = 196.9\ J \cdot K^{-1} \cdot mol^{-1}$ at the mean temperature of the vapor-pressure measurements, which yields $S^\circ_m(ZrF_4, g, 772.8\ K) = 413.8\ J \cdot K^{-1} \cdot mol^{-1}$ when combined with the entropy of the solid, being in excellent agreement with the statistical value $S^\circ_m(ZrF_4, g, 772.8\ K) = 414.7\ J \cdot K^{-1} \cdot mol^{-1}$.

Table 5 shows that while our third-law enthalpies are in reasonably good agreement with those derived from other vapor-pressure studies, the corresponding second-law values show considerable scatter. This point illustrates again that second-law results are much more prone to systematic errors, mainly in temperature measurement and from temperature gradients in the cell region, than are the absolute pressures; but when these sources of error are minimized and reliable second-law results can be obtained, the information is all the more valuable in corroborating the selected entropy and molecular constants, as shown here for ZrF_4.

The excellent agreement between the second- and third-law enthalpies of sublimation and the related agreement between the experimental second-law entropy and the statistically calculated value indicate a high degree of consistency for the results presented here. One can therefore have a similar high degree of confidence in the derived thermodynamic properties of $ZrF_4(g)$.

REFERENCES

1. Hildenbrand, D. L. *J. Chem. Phys.* **1964,** 40, 3438.
2. Hildenbrand, D. L. *Pure Appl. Chem.* **1988,** 60, 303.
3. Konings, R. J. M.; Booij, A. S.; Cordfunke, E. H. P. *Vibr. Spectrosc.* **1991,** 1, 383.
4. Konings, R. J. M.; Booij, A. S. *J. Chem. Thermodynamics* **1992,** 24, 1181.

5. Lau, K. H.; Cubicciotti, D.; Hildenbrand, D. L. *J. Chem. Phys.* **1977,** 66, 4532.
6. Clark, R. J. H.; Rippon, D. M. *J. Mol. Spectrosc.* **1972,** 44, 479.
7. Girichev, G. V.; Giricheva, N. I.; Malysheva, T. N. *Zh. Fiz. Khim.* **1982,** 56, 183; Petrov, V. M.; Girichev, G. V.; Giricheva, N. I.; Shaposhnikova, O. K.; Zasorin, E. Z. *Zh. Strukt. Khim.* **1979,** 20, 136.
8. Büchler, A.; Berkowitz-Mattuck, J. B.; Dugre, D. *J. Phys. Chem.* **1961,** 34, 2202.
9. Blander, M.; Morgan, H. W. cited in reference 8.
10. Whitman, C. I. *J. Chem. Phys.* **1952,** 20, 161.
11. Motzfeldt, K. *J. Chem. Phys.* **1955,** 59, 139.
12. Stern, J. H.; Gregory, N. W. *J. Phys. Chem.* **1957,** 61, 1226.
13. Lauter, S. cited in reference 18.
14. Sense, K. A.; Snyder, M. J.; Filbert, R. B., Jr. *J. Phys. Chem.* **1954,** 58, 995.
15. Cantor, S.; Newton, R. F.; Grimes, W. R.; Blankenship, F. F. *J. Phys. Chem.* **1958,** 62, 96.
16. Galkin, N. P.; Tumanov, Y. N.; Tarasov, V. I.; Shishov, Y. D. *Russ. J. Inorg. Chem.* **1963,** 8, 1054.
17. Akashin, P. A.; Belousov, V. I.; Sidorov, L. N. *Russ. J. Inorg. Chem.* **1963,** 8, 789.
18. Fischer, W.; Petzel, T. *Z. anorg. allg. Chem.* **1964,** 333, 226.
19. Sidorov, L. N.; Akishin, P. A.; Shol'ts, V. B.; Kotenev, Yu. M. *Russ. J. Phys. Chem.* **1965,** 39, 1146.
20. Westrum, E. F., Jr. *J. Chem. Eng. Data* **1965,** 10, 140.
21. McDonald, R. A.; Sinke, G. C.; Stull, D. R. *J. Chem. Eng. Data* **1962,** 7, 83.
22. Greenberg, E.; Settle, J. L.; Feder, H. M.; Hubbard, E. N. *J. Phys. Chem.* **1961,** 65, 1168.